



ELSEVIER

Journal of Nuclear Materials 282 (2000) 125–130

**Journal of
nuclear
materials**

www.elsevier.nl/locate/jnucmat

Retention of ion-implanted deuterium in tungsten pre-irradiated with carbon ions

V.Kh. Alimov ^{*,1}, K. Ertl, J. Roth, K. Schmid*Max-Planck-Institut für Plasmaphysik, Euratom Association, Boltzmannstr. 2, D-85748 Garching, Germany*

Received 4 May 2000; accepted 16 September 2000

Abstract

Deuterium (D) ion implantation and retention at room temperature was studied in pure and carbon (C) implanted tungsten single crystals. Pre-implantation with C was done at 40 keV and D implantation at 10 keV with the range confined in the carbon modified layer and at 100 keV with the range exceeding the carbon modified layer. The range distributions were investigated in situ using 1 MeV ^3He ions analysing the energy distributions of α particles from the $\text{D}(^3\text{He}, \text{p})\alpha$ reaction while the total amount of retained D was obtained from the p-integral. The range distribution of carbon was obtained from the backscattered ^3He energy distribution. C pre-implantation influences the D retention only if the range of the D ions is confined within the carbon modified surface layer. In this case, D diffusion beyond the ion range distribution does not occur and the retained D amount is smaller than in the pure W crystal. At D energies exceeding the carbon modified layer the retention occurs in the dislocation zone up to 1 μm and the total retained amount is the same for carbon implanted and pure W samples. © 2000 Elsevier Science B.V. All rights reserved.

1. Introduction

According to requirements and selection criteria in the ITER design, the plasma facing material will be chosen from beryllium, carbon fibre composite and tungsten. Physical and chemical sputtering causes erosion of plasma-facing materials and impurity release into the plasma. These elements and hydrogen from the plasma will subsequently be co-deposited back onto the wall and divertor surface, forming mixed layers. In view of the above mentioned fact, not only pure materials such as carbon (C), beryllium and tungsten (W) should be studied, but also carbides and carbon-containing materials.

Few data obtained by different experimental methods have been reported on deuterium (D) inventories in

tungsten after implantation of hydrogen isotope ions at energies in the range 0.1–8 keV [1–8]. It was shown that the hydrogen isotope inventory in W materials depends strongly on the material structure at temperatures in the range from 300 to 600 K [4]. More than 70% of the implanted deuterium diffuses into the bulk even at room temperature and is captured by lattice imperfections [4,6,7]. There is only few work on deuterium trapping in and thermal release from tungsten containing carbon, prepared by chemical vapour deposition (CVD) [9] or by annealing tungsten films kept in contact with carbon films at 1500–1673 K [10,11]. It was found that the amount of deuterium retained in $\text{W}_{85}\text{C}_{15}$ and $\text{W}_{60}\text{C}_{40}$ produced by CVD is more than double the value in CVD tungsten free from carbon atoms. In the tungsten layer containing carbon the concentration of retained D atoms is higher than that in pure tungsten by about 20% [10] and reaches the value of $\approx 1.5 \times 10^{28} \text{ m}^{-3}$ at room temperature [10,11]. The deuterium inventory in carbon-containing tungsten steeply decreases with increasing target temperature from 300 to 550 K and reaches the value of pure tungsten at higher temperatures [9]. No data on hydrogen solubility and diffusivity in tungsten carbides are available.

^{*} Corresponding author. Tel.: +7-095 330 2192; fax: +7-095 334 8531.

E-mail address: alimov@ipc.rssi.ru (V.Kh. Alimov).

¹ Present address: Institute of Physical Chemistry, Russian Academy of Sciences, Leninsky prospect 31, 17915 Moscow, Russia.

The present work was done to study the influence of preceding C ion implantation into tungsten on the retention of implanted deuterium.

2. Experimental

For the investigations a W-single crystal was used, 10 mm in diameter and 1.5 mm thick with a purity of 99.995 wt% produced by double electron-beam zone melting. The sample surface parallel to the (111) plane was mechanically and electrochemically polished.

The experiments were performed in the target chamber PHARAO which was used for both ion implantation and ion beam analysis [12,13]. The typical background pressure was better than 2×10^{-8} Pa. The target chamber is connected to a 100 keV implanter and a 2.5 MeV Van de Graaff accelerator providing different ion-beam analysis techniques. The implantation and analysis beams were applied to the sample through the same collimating system using different limiting apertures. The implantation with C or D ions was carried out through a fixed aperture 1.5 mm in diameter. In order to obtain a homogeneous fluence distribution the implantation beam was swept vertically over the implantation diaphragm. The ^3He analysing beam from the accelerator impinged onto the sample through an 1.0 mm aperture, which could be moved into a position concentric to the implantation aperture.

The implantation of carbon atoms into the W crystal was performed by bombardment of the sample with 40 keV C^+ beam at room temperature up to a fluence of $3 \times 10^{22} \text{ m}^{-2}$. The C ion current was 0.3 μA , equivalent to a flux density of C ions of about $1.0 \times 10^{18} \text{ m}^{-2} \text{ s}^{-1}$. For the convenience of the presentation, the W crystal implanted with C ions will be denoted below as W[C] sample. The deuterium implantation of the W crystal and the W[C] sample was performed at 300 K with 30 keV D_3^+ (10 keV D ions) and 100 keV D^+ at flux densities of $(3.2\text{--}3.7) \times 10^{18}$ and $(1.4\text{--}1.8) \times 10^{19} \text{ m}^{-2} \text{ s}^{-1}$, respectively.

The W crystal was analysed before and after implantation with C ions by Rutherford backscattering spectroscopy (RBS), using 1.0 MeV $^3\text{He}^+$ at normal incidence. The backscattered ^3He ions were energy analysed at a scattering angle of 165° by a surface barrier detector with a small opening angle of 2.88×10^{-4} sr. For detection of the random spectra the sample was rotated around $\langle 111 \rangle$ axis well off the channelling direction. The total charge of the incident ^3He ion beam used for the RBS measurement was 10 μC .

For the measurement of the deuterium depth profile the target was bombarded with 1.0 MeV ^3He ions and the α particles (primary energy 3.5 MeV) and protons from the $\text{D}(^3\text{He},\alpha)\text{H}$ nuclear reaction (NRA) were energy analysed by a small angle (1.03×10^{-3} sr) surface

barrier detector positioned at 75° to the sample normal (Fig. 1). The α particle spectrum was transformed into a depth profile of deuterium concentration with the computer program LORI [14] using nuclear cross section data measured by Möller and Besenbacher [15], and electronic stopping power data compiled by Ziegler [16]. Depth distributions could only be evaluated to a depth of about 500 nm due to overlapping signals from backscattering from W. Therefore, the proton signal (Fig. 1) was used to calculate the total retained deuterium atom areal density (D m^{-2}) in the near-surface layer of about 1 μm thickness. The integral of protons was calibrated against the α particle integral at equal analysing dose. Values of analysing beam dose times detector solid angle were obtained from the surface intensity of backscattered ^3He ions from the tungsten. The contribution of implanted carbon and deuterium to the electronic stopping power was taken into account. The total charge of the incident ^3He ion beam used for the NRA was usually 20 μC .

Since the carbon signal in the RBS spectra cannot be separated from the low energy part of the tungsten signal, the depth distributions of carbon atoms implanted into the tungsten crystal were determined indirectly comparing the high energy parts of measured RBS spectra for unimplanted and carbon implanted tungsten targets (Figs. 2(a) and (b)). In this region of the spectra the presence of carbon is reflected by a reduction of the tungsten RBS signal. The carbon distributions are evaluated in the framework of Bayesian probability theory with an adaptive approach. The procedure compares the measured RBS spectrum with a calculated ideal spectrum convoluted with a measured apparatus broadening function. The best estimate of the distribution reflects only the significant information in the data and contains no noise fitting. The procedure is described in detail in Toussaint et al. [17]. The carbon distribution providing the best fit of the experimental spectra is presented in Fig. 2(b).

3. Results and discussion

The analysis of the depth distributions of 40 keV C^+ implanted to a fluence of $3 \times 10^{22} \text{ m}^{-2}$ at room temperature is shown in Figs. 2(a) and (b). The extension of the implantation zone is about $(5\text{--}6) \times 10^{21} \text{ atoms m}^{-2}$, corresponding to 50–60 nm, if it is assumed that a tungsten carbide phase with an atomic density of about $9.7 \times 10^{28} \text{ atoms m}^{-3}$ is formed in this zone [18]. The maximum C atom concentration does not exceed 45%. According to TRIDYN calculations [19], however, the mean projected range of 40 keV C ions in W is about 45 nm and for the C ion fluence used in our experiments ($3 \times 10^{22} \text{ m}^{-2}$) the carbon depth profile is nearly constant up to a depth of ≈ 100 nm with a C concentration

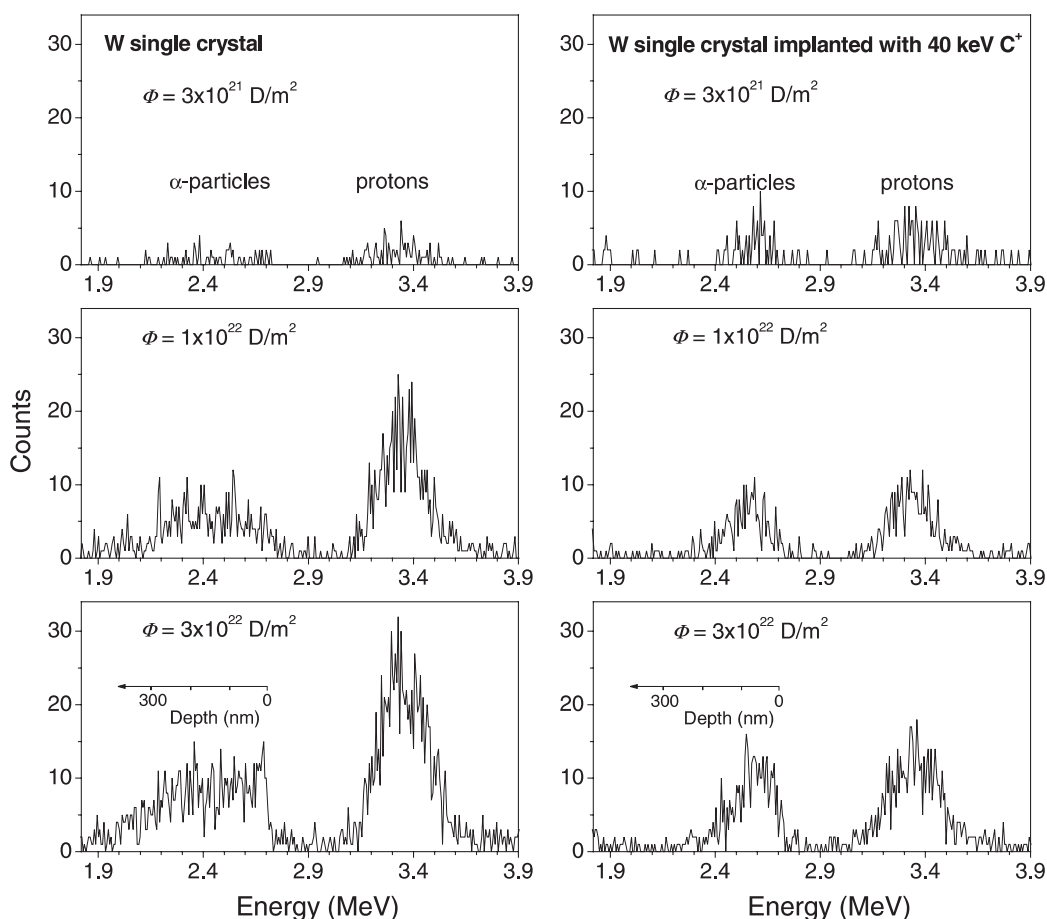


Fig. 1. Energy distributions of α particles and protons from the $D(^3\text{He}, \alpha)\text{H}$ reaction obtained from 1.0 MeV $^3\text{He}^+$ analysis of the W crystal and the carbon-containing W sample which were implanted with 10 keV D ions at 300 K up to the fluences indicated. The α particle distribution can be converted into a depth distribution of implanted D, while the proton signal gives the total retained amount.

of about 80%. From the comparison of the experimental and calculated results one must conclude that diffusion and phase formation effects occur which are not included in TRIDYN. The carbon concentration does not exceed that in a stoichiometric monocarbide WC phase. The higher reflection coefficient from WC compared to C [19] leads to a much smaller carbon retention than calculated neglecting carbide formation.

Deuterium ions were implanted into the W crystal and the W[C] sample at energies of 10 and 100 keV per deuteron. The calculated projected range of 10 keV D ions in W and WC carbide is 80 and 77 nm, respectively. Thus, D ions which are implanted into the W[C] sample at an energy of 10 keV are slowed down and create radiation damages practically in the same implantation zone as 40 keV C ions. In the case of 100 keV D ion implantation, deuterium is thermalized far beyond the C ion implantation zone.

Depth profiles of deuterium in the W crystal and in the W[C] sample irradiated with 10 and 100 keV D ions

at 300 K as obtained from Fig. 1 are given in Figs. 3 and 4. The variations of the amount of deuterium retained in the W crystal and the W[C] sample irradiated with D ions as determined from the proton counts are shown in Fig. 5 for the two D ion energies. Depth profiles of deuterium in the W crystal implanted with 10 keV D ions do not concur with the ion projected range distributions and are characterised by a maximum at a depth of 30–40 nm, a plateau reaching a depth of about 250 nm, and a gradual decrease with increasing depth. With the fluence increase the deuterium concentration in the maximum of the depth distribution reaches the value of $(6\text{--}7) \times 10^{27} \text{ m}^{-3}$ (Fig. 3) and practically does not change thereafter. At high fluences ($\geq 1 \times 10^{22} \text{ m}^{-2}$) a long tail of the D profile with a concentration of $(4\text{--}5) \times 10^{26} \text{ m}^{-3}$ extending beyond 400 nm is observed.

Deuterium implanted directly into the carbon-containing layer of the W[C] sample (the case of 10 keV D ion implantation) is accumulated practically in the near-surface layer ≈ 200 nm in thickness (recall that the

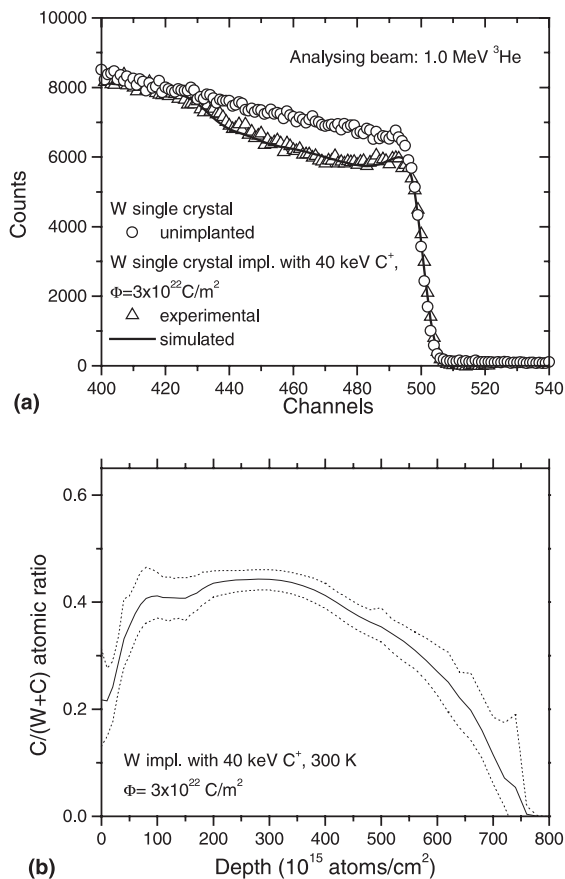


Fig. 2. *Top*: The measured and SIMNRA simulated backscattering spectra for 1.0 MeV ^3He ions incident on the W single crystal and the W crystal pre-implanted with 40 keV C^+ at room temperature to a fluence of $3 \times 10^{22} \text{m}^{-2}$. *Bottom*: Depth profile of 40 keV C^+ implanted into the W crystal as determined from the evaluation of Fig. 2(a) using Bayesian probability theory [17]. The dashed lines give the confidence interval of the evaluation.

carbon atoms are localised within a near-surface layer $\approx 100 \text{ nm}$ thick) and the deuterium profiles are localised in a Gaussian distribution (Fig. 3). In the case of 100 keV D ion implantation the concentration of deuterium in the W[C] sample is higher than that in the W crystal over the depth measured (50–450 nm) (Fig. 4). However, this depth interval is small compared to the ion range and total retention is very similar for pure and carbon pre-irradiated tungsten (Fig. 5).

As shown experimentally [4–6,10,20,21] and seen from Fig. 3, most of the deuterium implanted into pure tungsten at room temperature is trapped not only in the near-surface region of the sample, but significantly beyond the implantation range as well. The study of the damage structure produced in W crystals under D ion implantation by means of backscattering of MeV He

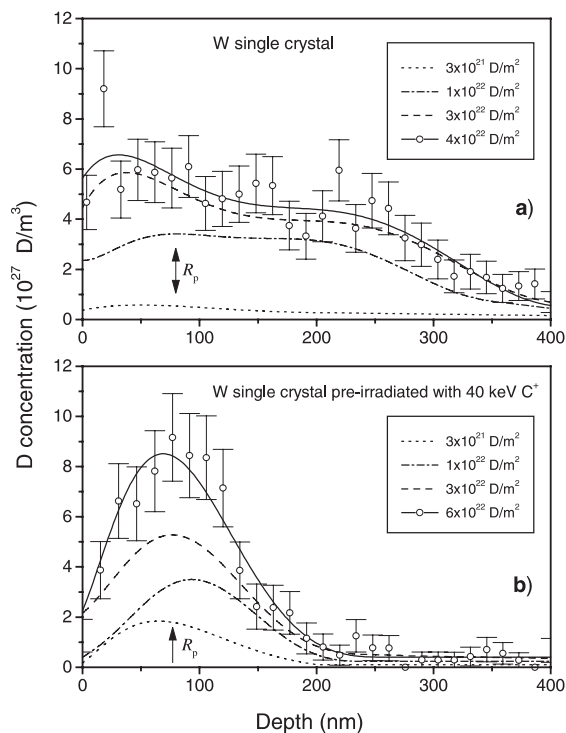


Fig. 3. Depth profiles of deuterium in the W crystal (top) and the carbon-containing W sample (bottom) implanted with 10 keV D ions at 300 K up to the fluences indicated as determined from the energy distributions of α particles from the $\text{D}(^3\text{He}, \alpha)\text{H}$ reaction using 1.0 MeV ^3He ions. The lines are polynomially smoothed fits to the data points (shown only for higher D ion fluence). The arrow indicates the mean projected range, R_p , of 10 keV D ions in W and WC carbide calculated by the TRIM.SP program [18].

ions in channelling geometry [10,20] and by measurement of D atom and D_2 molecule profiles using SIMS combined with RGA (residual gas analysis) [20,21] revealed that there are at least two types of defects which can be responsible for trapping of deuterium: (i) D_2 filled cavities localised in the implantation zone [20,21], and (ii) dislocations which are distributed practically uniformly from the surface to depth of $\approx 1 \mu\text{m}$ and capture deuterium in the form of D atoms [10,20,21]. For the W crystal irradiated with 10 keV D ions, the formation of D_2 molecules in the implantation zone starts at a fluence of $5 \times 10^{21} \text{m}^{-2}$ [21] when the D atom concentration reaches the value of $\approx 1 \times 10^{27} \text{atoms m}^{-3}$ ($\approx 1.5 \text{ at.}\%$). It should be noted that in the implantation zone two important conditions necessary for gas bubble formation are fulfilled: a high level of vacancy supersaturation and a high concentration of deposited deuterium.

The present data show that the concentration of D_2 molecules in the ion stopping zone at high fluences can reach a value of $(2\text{--}3) \times 10^{27} \text{molecules m}^{-3}$, whereas the

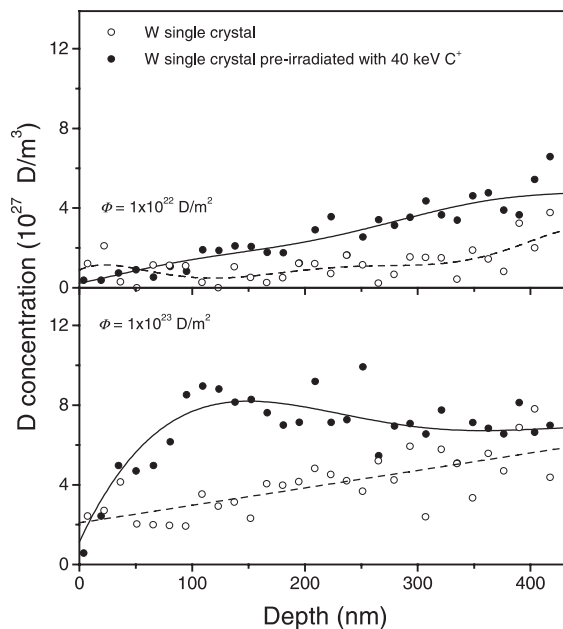


Fig. 4. Depth profiles of deuterium in the W crystal and the carbon-containing W sample implanted with 100 keV D ions at 300 K up to the fluences indicated as determined from the energy distributions of α particles from $D(^3\text{He}, \alpha)\text{H}$ reaction using 1.0 MeV ^3He ions. The lines are polynomially smoothed fits to the data points.

maximum concentration of D atoms trapped by dislocations at depths far beyond the ion range is of the order of $(0.6\text{--}1) \times 10^{27}$ atoms m^{-3} . It must be underscored that deuterium bubbles are also formed slightly beyond the implantation zone at a depth up to ≈ 350 nm (right shoulder in D depth distribution, see Fig. 3 top). A large part of the deuterium implanted into the W crystal diffuses into the bulk and is captured by structural defects, probably dislocations and, in polycrystal material, at grain boundaries. However, most of the implanted atoms diffuse to the crystal surface and is remitted after surface recombination [1,8,22].

As reported in Alimov [21], deuterium implanted into CVD monocarbide WC at room temperature is also accumulated in the form of both D atoms and D_2 molecules. With the increase of the ion fluence, the maximum concentrations of the atoms and molecules in the implantation zone reach values of $\approx 2 \times 10^{27}$ atoms m^{-3} and $\approx 3 \times 10^{27}$ molecules m^{-3} , respectively. Thus, ion-induced defects like cavities filled with D_2 rather than carbon atoms are of first importance in the trapping of deuterium in the stopping zone of the CVD monocarbide.

The concentration profile (Fig. 2) indicates that ion implanted carbon is not accumulated in the form of free atoms, but forms a carbide phase [18]. One would also speculate that initial irradiation of the W crystal with C

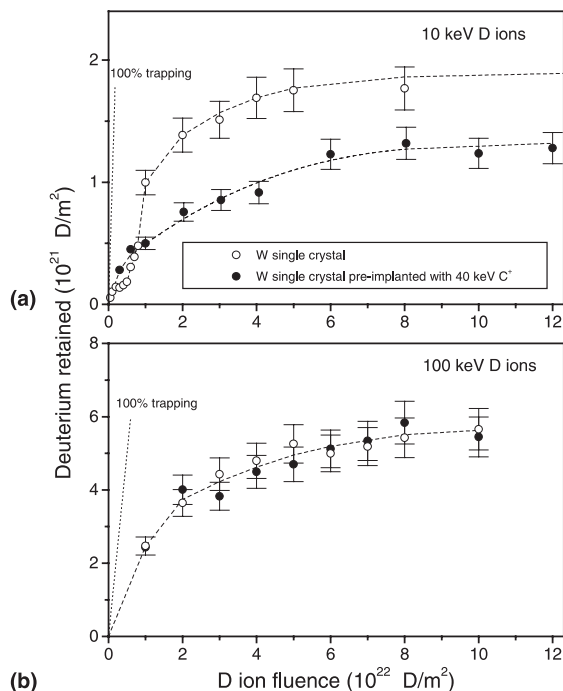


Fig. 5. Amount of deuterium retained at room temperature in the W crystal and the carbon-containing W sample as function of the D ion fluence at ion energies of 10 keV per deuteron (top) and 100 keV per deuteron (bottom) as determined from the integral of the proton counts.

ions leads to creation of dislocations both in the C ion implantation zone and far beyond, and that these defects could serve as traps for deuterium implanted subsequently. During further implantation closed pores and channels could be formed in the stopping zone of C ions. It is possible that deuterium is accumulated in the W-C layer as D atoms and D_2 molecules as well, though additional experiments are necessary for confirmation of this presumption. The comparison of deuterium concentrations at the depth of the D ion projected range in W-C layer and W crystal implanted with 10 keV D ion (Fig. 3) shows that the influence of carbon impurities on D retention is small. However, the profiles of deuterium implanted directly into W-C layer reflect the D ion range distributions with little diffusion to larger depth. This may be due to a smaller diffusion coefficient of D in WC than in pure W. However, another main parameter influencing the retention of implanted deuterium in tungsten samples is the surface recombination [22]. The C ion irradiation could lead to an increase of the recombination value and, therefore, to a decrease of the fraction of deuterium which diffuses into the bulk of the W[C] sample. In doing so the concentration of D atoms beyond the implantation zone is relatively small and is lacking for bubble formation.

The total retention of deuterium over a depth of about 1 μm is shown in Fig. 5. For 10 keV D ions characteristic differences for the W crystal and the W[C] samples are seen (Fig 5(a)). The retention in the W crystal initially is very low and increases strongly above fluences of $6 \times 10^{21} \text{ m}^{-2}$ indicating that a surface modification by radiation damage is necessary for deuterium retention. For the W[C] sample the deuterium retention is initially higher than in the W crystal but reaches a much lower saturation level. It should be noted that the retention of deuterium implanted directly into the W–C layer at low D ion fluences ($\leq 5 \times 10^{21} \text{ m}^{-2}$) is higher than that for pure tungsten (Fig. 5, retention curves for 10 keV D ions).

The majority of deuterium implanted into W and W[C] at an energy of 100 keV is accumulated in the bulk of the samples, therefore the contribution of deuterium trapped by defects created with C ions in the near-surface layer to the total D content is insignificant. That is the reason why the retention of deuterium implanted into the W[C] sample at energy of 100 keV is very similar to that for the W crystal (Fig. 5, retention curve for 100 keV D ions). In the case of 100 keV D ion implantation, the dislocations in the W[C] sample are thought to be responsible for trapping of deuterium ions which were implanted far beyond the C ion implantation zone.

4. Conclusions

The retention of deuterium in pure tungsten occurs in microcavities within the ion range and at dislocation type defects for diffusing deuterium atoms extending to depths up to 1 μm , i.e. well beyond the implantation zone [20,21]. Upon pre-implantation with carbon ions the deuterium retention is strongly influenced if the range of the deuterium ions is confined within the carbon modified surface layer. The total D retention is smaller in W[C] samples compared to pure W crystals and depth profiling shows that deuterium is only retained within the range distribution without diffusion beyond the carbon modified surface layer.

If the D ions are implanted at depths larger than the carbon modified layer thickness the difference to pure W crystals disappears. Close to the surface the retained deuterium in the carbon implanted layer is slightly higher, especially for high deuterium fluences, but diffusion beyond the ion range occurs as in pure tungsten. The total retained deuterium remains unchanged.

Acknowledgements

One of the authors, V.Kh.A., gratefully acknowledges financial support by the Max-Planck-Institut für

Plasmaphysik. The authors would like to thank Dr W. Eckstein for calculation of range distributions for deuterium implanted into W and WC carbide and Dr U. v. Toussaint for providing the program for evaluation of depth profiles from RBS spectra.

References

- [1] C. García-Rosales, P. Franzen, H. Plank, J. Roth, E. Gauthier, *J. Nucl. Mater.* 233–237 (1996) 803.
- [2] A.A. Pisarev, A.V. Varava, S.K. Zhdanov, *J. Nucl. Mater.* 220–222 (1995) 926.
- [3] R. Sakamoto, T. Mugora, N. Yoshida, *J. Nucl. Mater.* 233–237 (1996) 776.
- [4] V.Kh. Alimov, B.M.U. Scherzer, *J. Nucl. Mater.* 240 (1996) 75.
- [5] A.A. Haasz, J.W. Davis, *J. Nucl. Mater.* 241–243 (1997) 1076.
- [6] A.A. Haasz, J.W. Davis, M. Poon, R.G. Macaulay-Newcombe, *J. Nucl. Mater.* 258–263 (1998) 889.
- [7] A.A. Haasz, M. Poon, J.W. Davis, *J. Nucl. Mater.* 266–269 (1999) 520.
- [8] R. Causey, K. Wilson, T. Venhaus, W.R. Wampler, *J. Nucl. Mater.* 266–269 (1999) 467.
- [9] W. Wang, V.Kh. Alimov, B.M.U. Scherzer, J. Roth, *J. Nucl. Mater.* 241–243 (1997) 1087.
- [10] S. Nagata, K. Takahiro, S. Horiike, S. Yamaguchi, *J. Nucl. Mater.* 266–269 (1999) 1151.
- [11] T. Horikawa, B. Tsuchiya, K. Morita, *J. Nucl. Mater.* 258–263 (1998) 1087.
- [12] R. Siegele, J. Roth, B.M.U. Scherzer, S.J. Pennycook, *J. Appl. Phys.* 73 (1993) 2225.
- [13] R. Siegele, Relation between radiation damage and hydrogen trapping in graphite and silicon carbide, Technical Report IPP 9/87, Max-Planck-Institut für Plasmaphysik, Garching, 1991 (in German).
- [14] B.M.U. Scherzer, H.L. Bay, R. Behrisch, P. Borgesen, J. Roth, *Nucl. Instrum. and Meth.* 157 (1978) 75.
- [15] W. Möller, F. Besenbacher, *Nucl. Instrum. and Meth.* 168 (1980) 111.
- [16] J.F. Ziegler, Helium Stopping Power and Ranges in All Elemental Matter, in: *The Stopping and Ranges of Ions in Matter*, vol. 4, Pergamon, New York, 1977.
- [17] U.v. Toussaint, R. Fischer, K. Krieger, V. Dose, *New J. Phys.* 1 (1999) 11.
- [18] J. Luthin, Ch. Linsmeier, *Surf. Sci.* 454–456 (2000) 78.
- [19] W. Eckstein, Computer Simulation of Ion-Solid Interaction, Springer Series in Materials Science, vol. 10, Springer, Berlin, 1991.
- [20] V.Kh. Alimov, K. Ertl, J. Roth, K. Schmid, Deuterium retention and lattice damage in tungsten irradiated with D ions, in: Proc. 5th Int. Workshop on Hydrogen Isotopes in Solids, May, 2000, Stockholm, to be published in *Phys. Scripta*.
- [21] V.Kh. Alimov, Depth distribution of deuterium atoms and molecules in tungsten and tungsten monocarbide implanted with D ions (in preparation).
- [22] P. Franzen, C. García-Rosales, H. Plank, V.Kh. Alimov, *J. Nucl. Mater.* 241–243 (1997) 1082.